

Permeability of Cracked Steel Fiber-Reinforced Concrete

Julie Rapoport¹; Corina-Maria Aldea²; Surendra P. Shah, M.ASCE³; Bruce Ankenman⁴; and Alan Karr⁵

Abstract: This research explores the relationship between permeability and crack width in cracked, steel fiber-reinforced concrete. In addition, it inspects the influence of steel fiber reinforcement on concrete permeability. The feedback-controlled splitting tension test (also known as the Brazilian test) is used to induce cracks of up to 500 μm (0.02 in.) in concrete specimens without reinforcement, and with steel fiber reinforcement volumes of both 0.5 and 1%. The cracks relax after induced cracking. The steel fibers decrease the permeability of specimens with relaxed cracks larger than 100 μm .

DOI: 10.1061/(ASCE)0899-1561(2002)14:4(355)

CE Database keywords: Permeability; Cracking; Fiber reinforced materials; Concrete.

Introduction

Fiber-reinforced concrete is becoming an increasingly popular construction material due to its improved mechanical properties over unreinforced concrete and its ability to enhance the mechanical performance of conventionally reinforced concrete. Though much research has been performed to identify, investigate, and understand the mechanical traits of fiber-reinforced concrete, relatively little research has concentrated on the transport properties of this material.

Material transport properties, especially permeability, affect the durability and integrity of a structure. High permeability, due to porosity or cracking, provides an ingress for water, chlorides, and other corrosive agents. If such agents reach reinforcing bars within the structure, the bars corrode, thus compromising the ability of the structure to withstand loads, which eventually leads to structural failure.

Building codes require that cracks exposed to weathering be no larger than specified widths in order to ensure mechanical structural integrity. However, if cracks of this size significantly increase permeability and allow corrosive agents to reach steel reinforcement, the cracks are clearly too large and the codes should be revised. Knowledge pertaining to permeability can help determine the maximum allowable size of exposed cracks in

structures. In addition, if concrete casings are used as shielding containers for pollutants and toxic waste, permeability is of utmost importance in order to ensure that no potentially harmful leakage occurs.

Because of the important role played by permeability in structural safety, and the increasing use of fiber-reinforced concrete, this technical note examines the effects of different steel fiber volumes (0, 0.5, and 1%) in fiber-reinforced cracked specimens. Specimens were cracked to six different levels—0, 100, 200, 300, 400, and 500 μm —using the feedback-controlled splitting tension test, also known as the Brazilian test. The specimens were then tested for low pressure water permeability.

It was thought that increasing the volume of steel fibers would decrease the permeability of the cracked specimens due to crack stitching by the steel fibers. In addition, previous work performed by Aldea et al. showed that a permeability threshold exists for the crack width; cracks under 100 μm in cement paste, mortar, normal strength, and high strength concrete had little effect on permeability (Aldea et al. 1999). Cracks over 100 μm affected permeability significantly. It was expected that this threshold would still exist for the fiber-reinforced concrete because the steel fibers do not change the material porosity.

Experimental Methods

Three test series were investigated for permeability—concrete with no fibers (control), concrete with a steel fiber volume of 0.5% ($V_f=0.5\%$), and concrete with a steel fiber volume of 1% ($V_f=1\%$). Ordinary type I Portland cement was used. Washed, graded pea gravel with a 9.5 mm (3/8 in.) maximum size was used as coarse aggregates. River sand was used as fine aggregates. The steel fibers were manufactured by Bekaert and were 50 mm (2 in.) long, 0.5 mm (0.02 in.) in diameter, and had hooked ends. A small amount of superplasticizer was used. Table 1 shows the mix design for each test series. Each test series was cast into 100×200 mm (4×8 in.) cylinders, which were demolded after 24 h and cured at room temperature underwater in a 100% relative humidity room until the time of sample preparation. Samples were tested 8–10 months after casting.

¹Research Assistant, NSF Center for Advanced Cement-Based Materials, Northwestern Univ., 2145 Sheridan Rd., Evanston, IL 60208-4400.

²Materials Engineering Scientist, Saint Gobain Technical Fabrics, P.O. Box 728, St. Catharines ON, Canada L2R 6Y3.

³Director, NSF Center for Advanced Cement-Based Materials, Northwestern Univ., 2145 Sheridan Rd., Evanston, IL 60208-4400.

⁴Professor, Dept. of Industrial Engineering and Management Science, Northwestern Univ., 2145 Sheridan Rd., Evanston, IL 60208-4400.

⁵Associate Director, National Institute of Statistical Sciences, P.O. Box 14006, Research Triangle Park, NC 27709-4006.

Note. Associate Editor: Houssam A. Toutanji. Discussion open until January 1, 2003. Separate discussions must be submitted for individual papers. To extend the closing date by one month, a written request must be filed with the ASCE Managing Editor. The manuscript for this technical note was submitted for review and possible publication on December 11, 2000; approved on April 23, 2001. This technical note is part of the *Journal of Materials in Civil Engineering*, Vol. 14, No. 4, August 1, 2002. ©ASCE, ISSN 0899-1561/2002/4-355-358/\$8.00+\$5.00 per page.

Table 1. Mix Proportions by Weight, with Steel Fibers by Volume

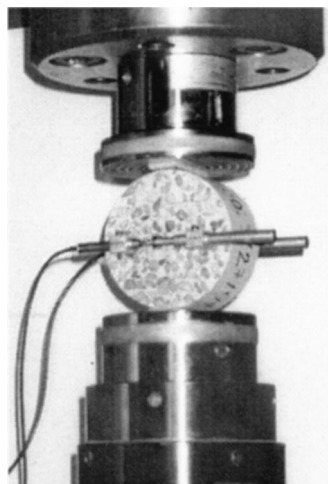
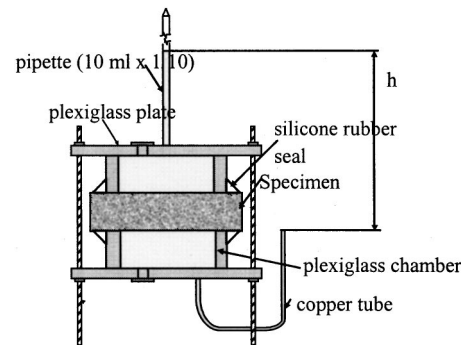
Mix	Cement	Water	Sand	Gravel	Super-plasticizer	Steel fiber volume
Control	1	0.45	2	2	0.006	—
Steel 0.5%	1	0.45	2	2	0.006	0.5%
Steel 1.0%	1	0.45	2	2	0.006	1.0%

Splitting Tension Test (Brazilian Test)

Specimens were cut to 50 mm (2 in.) in thickness with a circular saw. They were then cracked to a specified crack mouth opening displacement (CMOD) of 100, 200, 300, 400, or 500 μm using the Brazilian splitting tension test. Fig. 1 shows the experimental apparatus for the Brazilian test. A specimen was loaded in a 4.448 MN (1,000 kip) material test system (MTS) compressive testing machine, with a 489 kN (110 kip) load cell. A 100 \times 25 mm (4 \times 1 in.) strip of plywood was placed between the specimen and the steel platens on both the top and the bottom of the specimen to evenly distribute the load across the loading areas of the specimen. The Brazilian test compressed a circular specimen, which caused tensile stresses throughout the center region of the specimen. This induced cracking in the specimen (Wang et al. 1997). A strain gauge extensometer, with a maximum displacement of 0.5 mm (0.02 in.), or a linear variable differential transducer (LVDT), with a maximum displacement of 1 mm (0.04 in.), was attached to each face of the specimen to measure the crack width. The average displacement of the two strain gauges or LVDTs was used as a feedback signal to control the cracking. Cracks were induced at an opening rate of 0.1375 μs (0.00349 in./s) to the specified CMOD, and the loading and cracking histories were recorded. The strain gauges were used to induce cracks up to 300 μm . The LVDTs were used to induce the 400 and 500 μm cracks. After the cracks were induced, the specimens were unloaded and the cracks relaxed somewhat. The relaxation was measured.

Water Permeability Test

After the specimens were cracked, they were prepared for the water permeability test. Specimens were vacuum saturated following the procedure set forth in ASTM C 1202, the standard for the rapid chloride permeability test (ASTM 1994). Specimens were placed in a vacuum jar and pumped down to a vacuum of

**Fig. 1.** Brazilian splitting tensile test setup**Fig. 2.** Water permeability test setup

about 1 mm Hg for 3 h. Deionized water was then added to the jar and the vacuum was maintained for an additional hour, after which the vacuum pump was turned off. The specimens remained in the water for another 18 h.

After saturation, each specimen was removed to a water permeability test setup shown in Fig. 2, which is fully described by Wang et al. (1997). To test permeability, the system was filled with water. Additional water was added to the pipette. The water flowed through the concrete and out the copper tube. The change in water level in the pipette was used to calculate the water flow through the specimen, and thus the permeability of the material. After the initial water level in the pipette dropped by a specific amount, more water was added to the pipette with a syringe.

The initial permeability of the system was much higher than the final permeability. It is possible that the specimens were not perfectly saturated when the tests began. As such, water was run through the system until the permeability leveled off to an approximately constant value. In general, water was run through each specimen for about 24 h before data were taken. In specimens with large cracks, where the water flowed quite quickly, water had to be added to the system several times over these 24 h. Once the permeability seemed to reach a constant value, 10 readings were taken and averaged to find the permeability coefficient of the material.

The calculations to determine the permeability coefficient are detailed by Aldea et al. (1999). The water flow through the system is assumed to be continuous and laminar; therefore, Darcy's law can be applied. Because the flow is continuous, the amount of water flowing out of the pipette is shown to be

$$dV = A' \left(\frac{dh}{dt} \right) \quad (1)$$

where V = total volume of water that travels through the sample; A' = cross-sectional area of the pipette; h = head of water formed by the height of the chamber and water in the pipette; and t = time required for a certain amount of water to travel through the system.

Darcy's law states

$$Q = kA \frac{h}{l} \quad (2)$$

where Q = flow rate through the specimen (dV/dt); k = permeability coefficient and the parameter under study; l = thickness of the specimen; and A = cross-sectional area of the concrete.

By combining and integrating these equations, the permeability coefficient is found to be

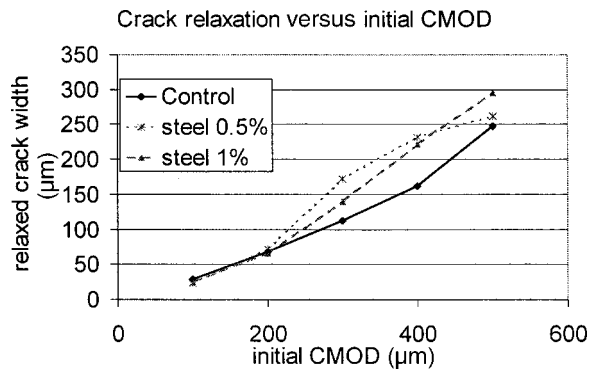


Fig. 3. Initial crack mouth opening displacement versus crack relaxation (average of two specimens for each point)

$$k = \left(\frac{A'l}{At} \right) \ln \left(\frac{h_0}{h_1} \right) \quad (3)$$

where h_0 and h_1 = heads of water at the beginning and end of the test, respectively. In addition, the theoretical flow rate of a liquid through a cracked material is found to be proportional to the cube of the crack width, which indicates that the permeability of a specimen with a larger crack will be much greater than that of a specimen with a smaller crack (Aldea et al. 2000).

Results and Discussion

Cracks were induced to a specified CMOD. The cracks then relaxed somewhat once they were unloaded. Fig. 3 shows the CMOD versus unloaded crack width for all three test series. Each data point is the average of the data from two specimens. The unreinforced concrete (no steel fibers) shows the most crack relaxation, where the cracks relaxed by about 62% on average. The cracks in the concrete with steel fibers seemed to relax less. This indicates that the fiber-reinforced concrete undergoes more inelastic (unrecoverable) deformation than the unreinforced concrete. The data shown in the following graphs are of permeability versus relaxed crack width.

Two specimens in each test series were cracked to each specified CMOD. The cracks relaxed and the samples were tested. The final CMOD after relaxation for each crack level was quite close for each treatment. The difference in CMOD of the relaxed cracks was generally no more than 5 μm for the 100 μm cracks, and 20 μm for the cracks larger than 100 μm . The data for each test series are shown in Fig. 4. Two features are of interest. The first is

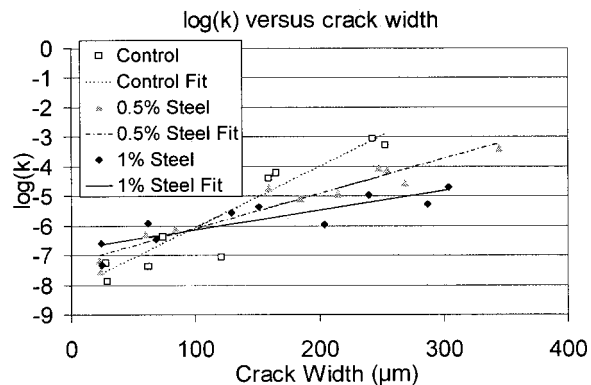


Fig. 4. Permeability versus crack width

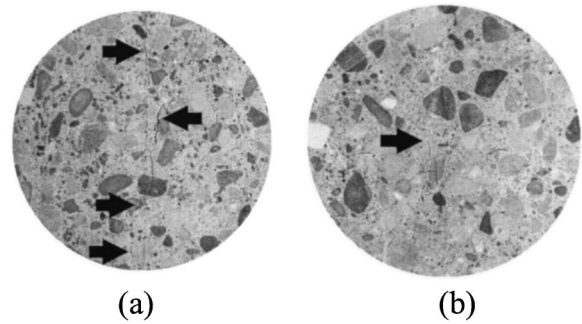


Fig. 5. Diagram of: (a) multiple cracking in steel 1% specimen cracked to 500 μm ; (b) single central crack in unreinforced specimen cracked to 500 μm

that, at higher levels of cracking, steel reinforcing fibers clearly reduce permeability. Further, the 1% steel fiber test series reduces permeability more than the 0.5% test series. This is most likely due to the stitching and multiple cracking effect that the steel fibers have. The steel fibers might stitch the cracks at the ends, perhaps shortening the length of the crack, and reducing the crack area for permeability.

In addition, the steel fiber reinforcement changes the crack geometry from one large crack to multiple smaller cracks. The steel fibers distribute the stress evenly throughout the material. Instead of the stress building around the biggest flaw and causing a large crack to open there, the stress builds around several flaws and causes several smaller cracks to open. Fig. 5(a) shows a steel 1% specimen cracked to 500 μm exhibiting multiple cracking. The cracks have been highlighted to make them easier to see. Fig. 5(b) shows a control (unreinforced) specimen, also cracked to 500 μm . Only one large, central crack is visible. Because permeability is related to the cube of the crack width, several smaller cracks will be less permeable than one large crack. Therefore, it is not surprising that steel fibers reduce the permeability of cracked concrete. It is possible that a higher fiber volume will further reduce the permeability of cracked concrete. However, at some fiber volume, an optimum might be reached, above which more fibers will increase permeability. Others have shown such optima to exist in microfiber reinforced concrete (Tsukamoto 1990; Tsukamoto and Wörner 1991).

The other feature of interest in Fig. 4 is that below a crack width of about 100 μm , steel reinforcing fibers do not seem to affect permeability much at all. Aldea et al. showed a similar occurrence with unreinforced concrete, mortar, and paste. This indicates that below cracks of 100 μm , reinforcing does not affect permeability (Aldea et al. 1999).

Statistical tests were performed on the slopes of the permeability lines shown on the semilog scale in Fig. 4. The tests found that the permeability of cracked concrete decreases with increasing fiber volumes. The tests are run at a 95% confidence level for cracks wider than 100 μm . For cracks smaller than 100 μm , the permeability difference is not statistically significant at the 95%

Table 2. Regression Results

Steel fiber level	Intercept	Standard error of the intercept	Slope	Standard error of the slope	Number of data points
Control	-8.1322	0.4462	0.020657	0.003064	10
0.5%	-7.2691	0.2181	0.011784	0.001097	10
1.0%	-6.8022	0.2482	0.006601	0.001381	10

Table 3. Confidence Intervals for Differences in Slopes

Comparison of slopes	Difference ($m_1 - m_2$)	Standard error of the difference ($\sqrt{s_1^2 + s_2^2}$)	df	$t_{0.025,df}$	Confidence interval of the difference
0.5% Steel-control	0.0089	0.0033	10.0	2.23	(0.0016, 0.0161)
1.0% Steel-0.5% Steel	0.0052	0.0018	15.7	2.13	(0.0014, 0.0089)

confidence level. A thorough explanation of the statistical test is located in the Appendix.

Conclusions

Two major conclusions can be drawn from this research.

1. At larger crack widths, steel reinforcing macrofibers reduce the permeability of cracked concrete. The higher steel volume of 1% reduces the permeability more than the lower steel volume of 0.5%, which is still lower than the permeability of unreinforced concrete. This is probably due to the crack stitching and multiple cracking effects of steel fiber reinforcement. The permeability differences above 100 μm in all test series are statistically significant at the 95% confidence level.
2. Below cracks of about 100 μm , steel reinforcing macrofibers do not seem to affect the permeability of concrete.

Acknowledgments

The research was performed at Northwestern University, the headquarters of the National Science Foundation (NSF)-Funded Center for Advanced Cement-Based Materials. Support from the NSF through grant DMS/9313013 to the National Institute of Statistical Sciences is greatly appreciated. The writers wish to thank Steve Hall, Steve Albertson, John Chirayil, and Joclyn Oats for their great help with sample preparation and apparatus design.

Appendix: Statistical Significance of Permeability Differences

For each fiber content, a regression line was fit to the log (base 10) of the permeability. Each data point and the three regression lines are plotted in Fig. 4. The regression provides a slope with a standard error and an intercept with a standard error for the three concrete mixes, each containing a different amount of steel fibers (Table 2).

As the amount of steel fibers increases, the slope of the regression line decreases, indicating that for large cracks (greater than about 100 μm), steel fibers reduce the permeability. To determine if the slopes of the regression lines are significantly different for the different amounts of steel fibers, confidence intervals were created for the difference between the slopes of the regression lines. A 95% confidence interval for the difference between two slopes, with standard errors m_1 and m_2 , respectively, is calculated as follows:

$$m_1 - m_2 \pm t_{0.025,df} \sqrt{s_1^2 + s_2^2}$$

The quantity $t_{0.025,df}$ is the 0.975 quantile of the t distribution with df degrees of freedom. If the regression for m_1 has n_1 data points and the regression for m_2 has n_2 data points, then

$$df = \frac{(s_1^2 + s_2^2)^2}{\left[\frac{s_1^4}{(n_1 - 2)} + \frac{s_2^4}{(n_2 - 2)} \right]}$$

The first row of Table 3 shows the confidence intervals for the difference between the slopes for plain concrete and concrete containing 0.5% steel fibers. The second row shows the confidence interval for the difference between the slopes for concrete containing 1.0% steel fibers and 0.5% steel fibers. Neither confidence interval contains zero, which confirms the conclusion that increasing the percentage of steel fibers in the concrete significantly (95% confidence) increases the slope of the lines.

The regression lines cross at about 100 μm , suggesting that below 100 μm , the addition of steel fibers actually increases the permeability. However, when confidence intervals for the differences between the intercepts of the regression lines are calculated, the differences in the intercepts are not significantly different from zero. Therefore, it is reasonable to conclude that steel fibers actually have little or no effect on the permeability of concrete with cracks smaller than 100 μm .

Notation

The following symbols are used in this technical note:

- A = concrete specimen cross-sectional area;
- A' = pipette cross-sectional area;
- df = degrees of freedom;
- h = water head;
- h_0 = initial water head;
- h_1 = final water head;
- k = permeability coefficient;
- l = specimen thickness;
- m = standard error of slope;
- Q = flow rate;
- t = time required for water to travel through sample; and
- V = total volume of water that travels through sample.

References

- Aldea, C.-M., Gandehari, M., Shah, S. P., and Karr, A. (2000). "Estimation of water flow through cracked concrete under load." *ACI Mater. J.*, 97(5), 567–575.
- Aldea, C.-M., Shah, S. P., and Karr, A. (1999). "Permeability of cracked concrete." *Mater. Struct.*, 32, 370–376.
- ASTM. (1994). "Standard method for electrical indication of concrete's ability to resist chloride ion penetration." *C 1202-94*, West Conshohocken, Pa.
- Tsukamoto, M. (1990). "Tightness of fibre concrete." *Darmstadt Concr. Annu. J. Concr. Concr. Struct.*, 5, 215–225.
- Tsukamoto, M., and Wörner, J.-D. (1991). "Permeability of cracked fibre-reinforced concrete." *Darmstadt Concr. Annu. J. Concr. Concr. Struct.*, 6, 123–135.
- Wang, K., Jansen, D. C., and Shah, S. P. (1997). "Permeability study of cracked concrete." *Cem. Concr. Res.*, 27(27), 381–393.